PCCP

Third virial coefficients and critical properties of quadrupolar two center Lennard-Jones models†

L. G. MacDowell,*[a] C. Menduiña,[a] C. Vega[a] and E. de Miguel[b]

[a] *Dpto. de Química Física, Facultad de Ciencias Químicas, Universidad Complutense, 28040, Madrid, Spain. E-mail: luis@ender.quim.ucm.es*
[b] *Dpto. de Física Aplicada, Facultad de Ciencias Experimentales, Universidad de Huelva, 21071, Huelva, Spain*

Received 11th March 2003, Accepted 1st May 2003
First published as an Advance Article on the web 28th May 2003

We report numerical results for the third virial coefficient of two center Lennard-Jones quadrupolar molecules. Calculations are performed for 35 models with different elongations and quadrupoles over a temperature range from half to twice the critical temperature. It is found that increasing the elongation at fixed quadrupole has the effect of increasing B_3. On the other hand, at fixed elongation B_3 first decreases with increasing quadrupole at low temperatures, then increases with increasing quadrupole at higher temperatures. We estimate the temperature at which the third virial coefficient vanishes. Although both this temperature and the critical temperature increase with the quadrupole moment, their ratio remains almost constant. We predict the critical properties using two different truncated virial series. The first one employs the exact second and third virial coefficients. The second one approximates the fourth order contribution by using estimates obtained for hard diatomics. It is found that both methods yield fairly good predictions, with a somewhat better performance of the approximate fourth order expansion. The two methods are complementary, however, because they consistently bracket the exact value as determined from computer simulations.

I. Introduction

The virial expansion provides one of the most useful and theoretically sound equations of state for low density gases.[1,2] According to this equation, the pressure of a fluid may be expressed as a power series in the density, and the coefficients in the expansion are known as the virial coefficients. One of the most interesting aspects of the virial expansion is that the virial coefficients may be exactly related to the intermolecular potential.[3] Accordingly, experimental measurements of these coefficients provide important insight into the nature of intermolecular forces. Indeed, for a long time the measurement of second virial coefficients provided one of the few sources that allowed to test two body forces.[1] Although in principle a study of third virial coefficients could provide a means for the understanding of three body forces,[4,5] such studies have been considerably limited, for several reasons. Firstly, the experimental measurement of third virial coefficients has proved to be extremely difficult, due to instrumental and technical difficulties. Secondly, numerical calculations involve multidimensional integration and very time consuming computer calculations. Thirdly, two body forces need to be known accurately for any information on the three body forces to be extracted.

For these reasons, the study of third and higher order virial coefficients has either been limited to very simple realistic potentials, such as the Lennard-Jones[6–8] or to idealized model potentials, such as hard bodies. In the case of hard body potentials, the situation is simpler, because there exist useful analytic or approximate methods that allow to obtain theoretical estimates.[9,10] In other instances, analytic estimates are unavailable, but the hard nature of the potential makes numerical calculations much easier, for two reasons: Firstly, the potentials are short range, so that the integral bounds are small; secondly, the Mayer function adopts only two possible values, either -1 or 0, so that sampling the integrand yields results with a relatively small variance. This property is very important, because in practice most high order virial coefficients are determined numerically by means of Monte Carlo methods,[11] rather than standard quadrature methods. As a result, it has been possible to calculate high order virial coefficients for hard body potentials of very complicated models such as polymers.[12–15]

Despite the difficulties related to the measurement and calculation of third virial coefficients, there has been recently a growing interest in this issue, as a result of several reasons. Firstly, the improvement of the Burnett technique has allowed to measure third virial coefficients with a precision that was not possible until recently.[16] Secondly, the increase in computer power allows now to determine third virial coefficients numerically in a reasonable amount of time, with error bars similar to or smaller than those attained experimentally.[17–20] It has also been recently recognized that knowledge of the first few virial coefficients may allow for the development of equations useful in the field of supercritical extraction.[19,21,22] Finally, another observation that has partially motivated this work is the fact that a truncated virial expansion may allow to give rather accurate estimates for the critical properties of pure fluids. This observation was already employed a long time ago in order to estimate the critical properties of the Lennard-Jones fluid,[8] and other more complicated fluids, such as the Gay-Berne,[23] the dipolar hard sphere,[18] or water.[20] More recently, Boublik and Janecek have presented an interesting way of extending the series up to fourth order, with promising results.[24,25]

† Electronic supplementary information (ESI) available: third virial coefficients for quadrupolar two center Lennard-Jones models. See http://www.rsc.org/suppdata/cp/b3/b302780e/

Recently, some of us have been involved in the systematic calculation of second virial coefficients of diatomic molecules. We have made calculations for different bond lengths and multipole moments, for both pure fluids and their mixtures.[26,27] The second virial coefficients of multi center models describing fullerenes have also been studied recently.[28] In this work, we extend our previous calculations. We will present results for the third virial coefficient of quadrupolar diatomic molecules. Each of the sites within the molecule will be modeled with a Lennard-Jones potential, which may either represent a single atom, such as in N_2, or a "united atom", such as in the case of ethane, CH_3–CH_3 or ethylene, CH_2=CH_2. Our results provide a large data base for third virial coefficients which allows to study the dependence of these property on several molecular parameters such as bond length and quadrupole moment or state variables such as temperature. It will also allow to test the performance of the virial series as a means to estimate critical properties, since extensive computer simulations are available[29] which will allow to test our results.

The organization of the paper is as follows. Firstly we will describe the molecular model employed and the numerical methodology required to calculate the third virial coefficient. In the next section, we will present our results and discuss the main trends observed. Also in this section we estimate the critical properties as obtained from the truncated virial expansion. Finally, in section IV we will summarise our results and present our conclusions.

II. Model and calculation details

Our model consists of two Lennard-Jones interaction sites a distance L apart and a point quadrupole in the center of the molecular axis. Accordingly, the full potential acting between a pair of molecules is given as follows:

$$u(1,2) = \sum_{i=1}^{2}\sum_{j=1}^{2} u_{ij}^{\mathrm{LJ}}(1,2) + u_{QQ}(1,2) \tag{2.1}$$

The u_{ij} are site–site Lennard-Jones potentials which only depend on the distance, d_{ij} between the sites,

$$u_{ij}^{\mathrm{LJ}} = 4\varepsilon\left\{\left(\frac{\sigma}{d_{ij}}\right)^{12} - \left(\frac{\sigma}{d_{ij}}\right)^{6}\right\} \tag{2.2}$$

The u_{QQ} term is a quadrupole potential which depends on the total quadrupole moment, Q, the distance between the center of the molecules, r_{12}, and their relative orientation. In Gaussian units, we have:[30]

$$u_{QQ} = \frac{3Q^2}{4r_{12}^5}\left(1 - 5\left(c_1^2 + c_2^2 + 3c_1^2c_2^2\right) + 2(s_1s_2c_{12} - 4c_1c_2)^2\right) \tag{2.3}$$

where $c_i = \cos\theta_i$, $s_i = \sin\theta_i$ and $c_{12} = \cos(\phi_2 - \phi_1)$, while θ_i and ϕ_i are the polar and azimuthal angles required to specify the orientation of molecule i (the reader is addressed to Fig. 1 of ref. 26 for further details on the evaluation of the quadrupolar potential). Since the quadrupole potential shows a divergence for molecules whose center of mass coincides, the Lennard-Jones interaction sites are embedded by hard spheres of diameter $1/\sqrt{2}$. This avoids overflow of the Mayer functions for overlapping molecules.

The third virial coefficient of linear molecules interacting by means of a pairwise additive potential is given by the following equation:[1,30]

$$B_3(T) = -\frac{1}{3V}\iiint \langle f_{12}f_{13}f_{23}\rangle_{\omega_1,\omega_2,\omega_3}\,\mathrm{d}\boldsymbol{r}_1\,\mathrm{d}\boldsymbol{r}_2\,\mathrm{d}\boldsymbol{r}_3 \tag{2.4}$$

where $\langle\ldots\rangle_{\omega_1,\omega 2,\omega 3}$ denotes an unweighted average over molecular orientations:

$$\langle\ldots\rangle_{w_i} = \frac{1}{4\pi}\int\ldots\mathrm{d}\theta_i\mathrm{d}\phi_i \tag{2.5}$$

while f_{ij} is the Mayer function:

$$f_{ij} = \exp(-\beta u(i,j)) - 1 \tag{2.6}$$

In the above equation, $\beta = (k_{\mathrm{B}}T)^{-1}$, with k_{B} Boltzmann's constant and T the temperature.

For linear systems as the ones considered here, where each orientation is specified by means of two degrees of freedom, eqn. (2.4) shows that in principle the calculation of B_3 involves a 15 dimensional integral. Fortunately, the Hamiltonian is invariant with respect to translation and rotation, so that only nine coordinates are required to specify the complete set of non-equivalent configurations. In order to specify each of these configurations we proceed as follows. First, we place molecule 1 at the origin of the laboratory reference frame and set the x and z axis such that the molecule lies in the xz plane. In this way, only a polar angle, θ_1, is required to determine the orientation of molecule 1. Secondly, we place the center of molecule 2 along the z axis, so that overall we need three coordinates to specify the relative position of this molecule: The distance of the center from the origin, r_{12}, together with one polar and one azimuthal angle, θ_2 and ϕ_2, respectively. Finally, the center of molecule 3 is located by means of a set of polar coordinates, r_{13}, Θ_3, Φ_3, while its orientation is specified by means of another set of polar and azimuthal angles, θ_3 and ϕ_3. With this choice of coordinates, we can now integrate the six trivial degrees of freedom to get the following simplified expression:

$$B_3 = -\frac{1}{3}\frac{2^3\pi^2}{(4\pi)^3}\iiint f_{12}f_{13}f_{23}\;\mathrm{d}\boldsymbol{q}_1\,\mathrm{d}\boldsymbol{q}_2\,\mathrm{d}\boldsymbol{q}_3 \tag{2.7}$$

where $\boldsymbol{q}_i$ are vectors specifying the coordinates of each molecule:

$$\mathrm{d}\boldsymbol{q}_1 = \mathrm{d}\cos\theta_1 \tag{2.8}$$

$$\mathrm{d}\boldsymbol{q}_2 = r_{12}^2\,\mathrm{d}r_{12}\mathrm{d}\cos\theta_2\mathrm{d}\phi_2 \tag{2.9}$$

$$\mathrm{d}\boldsymbol{q}_3 = r_{13}^2\mathrm{d}r_{13}\mathrm{d}\cos\Theta_3\mathrm{d}\Phi_3\,\mathrm{d}\cos\theta_3\,\mathrm{d}\phi_3 \tag{2.10}$$

Although the dimensionality of the problem has been reduced from 15 to 9, it is still too high for standard quadrature methods to be useful. In this work we evaluate B_3 by means of the well known Monte Carlo method.[11] In this way, our final working expression becomes:

$$B_3 = -\frac{1}{3}2^4\pi^2r_{\mathrm{c}}^2\frac{1}{N_{\mathrm{t}}}{\sum_{N_{\mathrm{t}}}}'f_{12}f_{13}f_{23}r_{12}^2r_{13}^2 \tag{2.11}$$

where r_{c} is some suitably chosen distance beyond which the Mayer function may be considered to be essentially zero, N_{t} is the total number of function evaluations and the prime next to the sum indicates that the molecular configurations are sampled randomly such that r_{12} and r_{13} are chosen uniformly in the interval $[0,r_{\mathrm{c}}]$; ϕ_2, ϕ_3 and Φ_3 are chosen uniformly in the interval $[0,2\pi]$; and $\cos\theta_1$, $\cos\theta_2$, $\cos\theta_3$, $\cos\Theta_3$ are chosen uniformly in the interval $[-1,1]$.

The calculations were divided into a set of independent blocks. In this way, B_3 could be given as an average of the independent runs, and the error estimated from the standard deviation of the sample. As the problem is very time consuming we used a parallelised code, dividing the load of integrand evaluations between the available processors. Typically, we employed 200 blocks and about 4×10^6 integrand evaluations per block and processor in a Pentium III dual machine running at 700 MHz. This implied about 1600×10^6 integrand evaluations per virial coefficient, or equivalently, one hour of cpu time per processor for each virial coefficient.

Table 1 Results for the third virial coefficient of a model with bond length $L = 0.6$. ΔB_3 stand for error bars obtained as $1/\sqrt{N_t}$ times the standard deviation of the mean

Q^2	T	B_3	$\pm\Delta B_3$
0.0	2.59147	8.54	0.01
1.0	2.03307	7.83	0.02
2.0	1.89797	2.95	0.04
3.0	1.77780	−13.6	0.1
4.0	1.43040	−341	1.0

The accuracy of the calculations depends on two parameters. On the one hand, N_t controls the statistical error, while on the other hand, r_c controls the systematic error related with truncation of the potential. These two parameters show a coupling, however, because the larger r_c, the larger the statistical error. We have investigated the dependence of B_3 on the value of r_c for a fixed value of N_t. We found that for r_c larger than 5σ, the resulting statistical error bars increased such that they did not allow us to observe any significant difference between the data. We have therefore evaluated all our data for a truncation value of $r_c = 5\sigma$. We recall that the cutoff is implemented in a center of molecule–center of molecule basis, rather than on a site–site basis. The error is temperature dependent. The higher the temperature, the smaller the error. The reason is that at high temperatures the Mayer function tends to a Heaviside function, which takes only two possible values. On the contrary, at low temperature the Mayer function shows a sharp peak, which results in a large variance of the values the integrand can take. At any rate, with our choice of N_t and r_c the statistical error bars are typically about 0.1% and exceed 1% only where B_3 vanishes.

We have checked our code by comparing the results with the literature on the Lennard-Jones fluid,[7,31] and the Stockmayer fluid,[4] as well as for hard[10] and square-well[32] dumbbells, and Lennard-Jones diatomics.[21] Excellent agreement with the cited references was obtained in all cases. In order to allow for cross checking, Table I shows results obtained from our code for a model with $L/\sigma = 0.6$ and different quadrupoles. The error bars are in all cases significantly smaller than 1%.

III. Results and discussion

Before starting a discussion of the results, we note that all throughout this section the different properties will be given in terms of Lennard-Jones units, which imply the following transformations: $T \to k_B T/\varepsilon$, for the temperature; $p \to p\sigma^3/\varepsilon$, for the pressure, $\rho \to \rho\sigma^3$ for the density; $B_3 \to B_3/\sigma^6$ for the third virial coefficient, $L \to L/\sigma$ for the bond length and $Q^2 \to Q^2/(\varepsilon\sigma^5)$ for the squared quadrupole.

We have calculated third virial coefficients for seven different elongations, $L = 0$, 0.2, 0.4, 0.5, 0.6, 0.8, 1.0 and five quadrupole moments, $Q^2 = 0$, 1, 2, 3, 4. The non-linear scale employed to describe the quadrupole range may seem somewhat odd at first sight, but it is common practice in simulations,[29] the reason being that the quadrupolar energy is linear in Q^2 (*cf.* eqn. (2.3)). Also note that the results for $L = 0$ refer to a single site model, not to a two site model. For each elongation and quadrupole we have determined virial coefficients for 20 temperatures ranging between 1/2 and 2 times the critical temperature. For the critical temperatures we employed estimates obtained by Stoll *et al.* using the NpT plus test particle method.[29] The choice of elongations and quadrupoles actually follows that employed by Stoll *et al.* This will allow us to compare the predictions of critical properties from the virial series with their simulation results. Furthermore, the range $L = [0,1.0]$ and $Q^2 = [0,4]$ is physically meaningful. Recently, Vrabec *et al.* were able to fit very accurately the vapor–liquid equilibria of more than 20 substances, including all the halogens, nitrogen, carbon dioxide, ethane, ethene and ethyne, with molecular parameters within the chosen range.[33] The choice of L allows to describe both monoatomic fluids ($L = 0$) and rather elongated linear molecules, such as CO_2 ($L \approx 0.8$). The range of quadrupoles also allows to consider most simple quadrupolar molecules. For example, Vrabec *et al.* could fit the properties of molecules with a wide range of absolute quadrupoles using reduced quadrupoles within the range $Q^2 = [0, 4]$,[33] *e.g.*, C_2H_6 with $Q^2 = 0.07$; I_2 with $Q^2 = 0.878$, N_2 with $Q^2 = 1.07$, Cl_2 with $Q^2 = 1.78$; and CO_2 with $Q^2 = 3.3$. All the results obtained in this work are available as electronic supplementary information (ESI).†

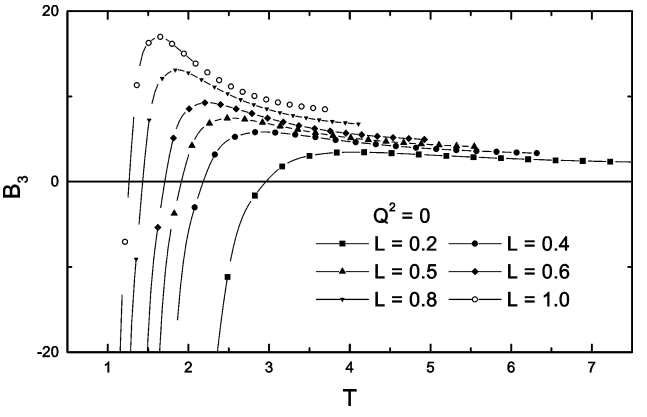

Fig. 1 Third virial coefficient as a function of temperature for zero quadrupole and different elongations. The symbols are numerical results, and the lines are a guide to the eye.

Let us first consider the influence of the molecular elongation on the third virial coefficient. In Fig. 1 we plot B_3 as a function of temperature for models with $Q^2 = 0$ and different elongations. In all cases, B_3 is seen to be negative at low temperature, then increases up to a maximum and then gradually decreases. This trend is similar to that observed for the Lennard-Jones fluid[31] and other simple fluids.[1] Both the temperature at the maximum and the temperature at which B_3 vanishes decrease as L increases. In all cases, B_3 seems to increase with L at a given temperature. A similar plot for the largest quadrupole studied, $Q^2 = 4$, is shown in Fig. 2. The observed trends are seen to be qualitatively similar to those observed for apolar molecules, although the maximum is clearly shifted to higher temperatures.

Let us now consider the influence of the quadrupole moment at fixed elongation. Fig. 3 shows a plot of B_3 as a function of temperature for different values of Q^2. At fixed elongation and temperature, B_3 is seen to decrease with increasing quadrupole.

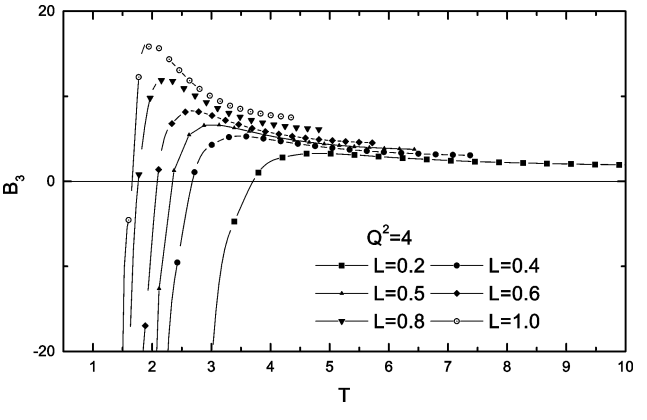

Fig. 2 Third virial coefficient as a function of temperature for $Q^2 = 4$ and different elongations. The symbols are numerical results, and the lines are a guide to the eye.

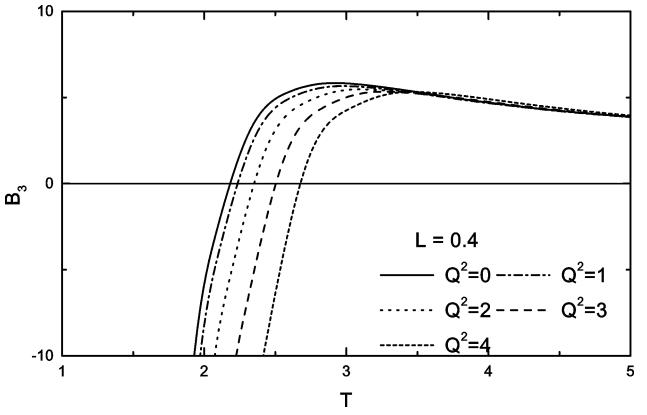

Fig. 3 Third virial coefficient as a function of temperature for $L = 0.4$ and different quadrupole moments.

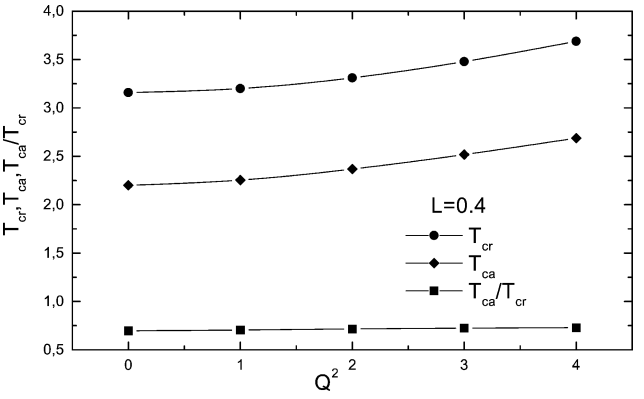

Fig. 5 Plot of the critical temperature, T_{cr}, the temperature at which B_3 vanishes, T_{ca}, and their ratio, as a function of quadrupole moment for $L = 0.4$.

Although the quadrupole interactions averaged over all orientations vanish, this is not the case for the averaged Boltzmann factor, which favors molecular orientations such that the interactions are attractive. For this reason, adding a quadrupole has the effect of increasing the cohesive interactions between molecules, resulting in a decrease of B_3. At temperatures well beyond the maximum, however, B_3 becomes almost independent of the quadrupole. Clearly, at this high temperatures βu_{QQ} becomes negligible, so that no particular molecular elongations are favored and the molecules no longer feel the effect of Q^2. Within these low and high temperature regimes, there appears a region where B_3 increases with increasing quadrupole moment, but the reason for this crossover is not clear. In Fig. 4 we show a similar plot for $L = 0.8$. The trend found is similar to that observed for $L = 0.4$, the main difference being a shift of the maximum to lower temperatures. Also note that the region were B_3 increases with increasing quadrupole moment becomes larger.

Since the qualitative shape of B_3 as a function of temperature is similar for all models, one can characterize the curve by means of a single temperature describing one salient feature of the curve $B_3 = B_3(T)$. Two such choices could be the temperature where the maximum occurs or the temperature at which B_3 vanishes. For the second virial coefficient, it is standard to discuss the Boyle temperature, T_b, where $B_2 = 0$. Accordingly, in this work we will discuss the temperature at which $B_3 = 0$. In order to avoid confusion with the critical temperature, T_{cr}, we denote this temperature T_{ca}.

In Fig. 5 we plot T_{cr} and T_{ca} for fixed elongation, $L = 0.4$ and different quadrupoles (T_{cr} obtained from ref. 29). The figure shows that T_{cr} is always larger than T_{ca}, *i.e.*, at least for the models considered in this work B_3 is always positive at the critical point. It is also seen that both T_{cr} and T_{ca} monotonously increase with Q^2. The ratio T_{ca}/T_{cr}, however, is seen to be an almost flat function of the quadrupole, with a value of about 0.7. Fig. 6 shows similar results for $L = 0.8$. As previously, T_{cr} is found to be always larger than T_{ca}, while the ratio T_{ca}/T_{cr} is seen to be a smooth function, ranging from about 0.70 to 0.75 for a wide range of quadrupole moments.

It is also interesting to compare T_{cr} and T_{ca} with the Boyle temperature, T_b, which we have calculated for quadrupolar Lennard-Jones diatomics in previous work.[26] In Fig. 7 we show the ratio of T_b/T_{ca} and T_b/T_{cr} as a function of quadrupole moment for fixed elongation, $L = 0.4$, together with the ratio T_{ca}/T_{cr} for comparison. The figure shows that T_b is always larger than T_{ca}, implying that B_3 always becomes positive before B_2. Similarly, T_b/T_{cr} is always larger than unity, so that B_2 is always negative at the critical temperature. The ratio T_b/T_{cr} is less useful than the ratio T_{ca}/T_{cr} as a predictive tool for T_{cr}, however, since the latter is found to be more smooth. In order to show that these trends are not particular to a given elongation, we present similar results for $L = 0.8$ (Fig. 8). The figure shows indeed that the trends observed for $L = 0.4$ are also obeyed in this case.

Table 2 collects the value of T_{ca} for the 35 models studied in this work. The table shows that the change of T_{ca} with molecular parameters is smooth, except for $L = 0$. The reason for this difference is that the model with $L = 0$ is actually the Lennard-Jones fluid, *i.e.*, it has only one site, while all the other models with $L > 0$ have two sites (note that the properties of a two site model with $L = 0$ may be trivially related to those of a one site Lennard-Jones model).

A useful application of the virial coefficients is the prediction of critical properties. Vliegenthart *et al.* have shown that the

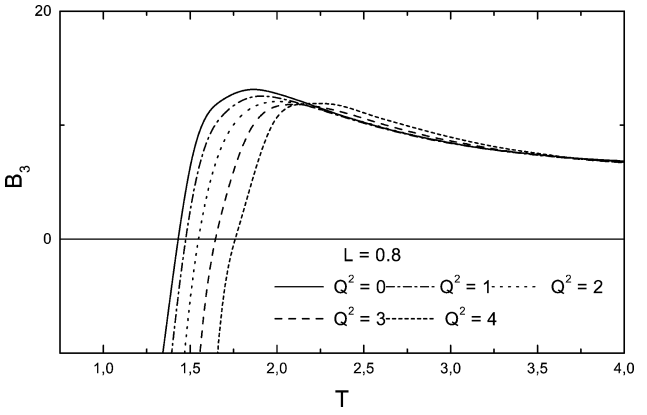

Fig. 4 Third virial coefficient as a function of temperature for $L = 0.8$ and different quadrupole moments.

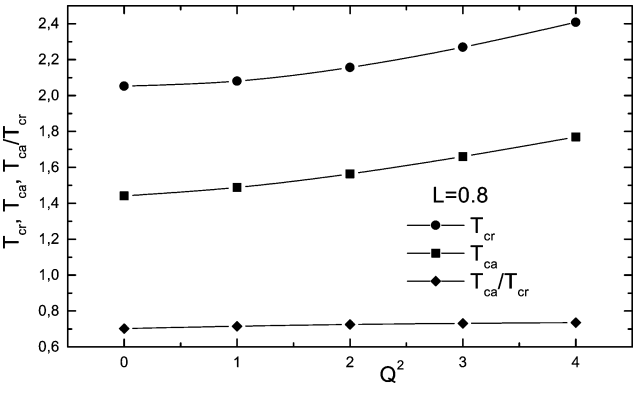

Fig. 6 Plot of the critical temperature, T_{cr}, the temperature at which B_3 vanishes, T_{ca}, and their ratio, as a function of quadrupole moment for $L = 0.8$.

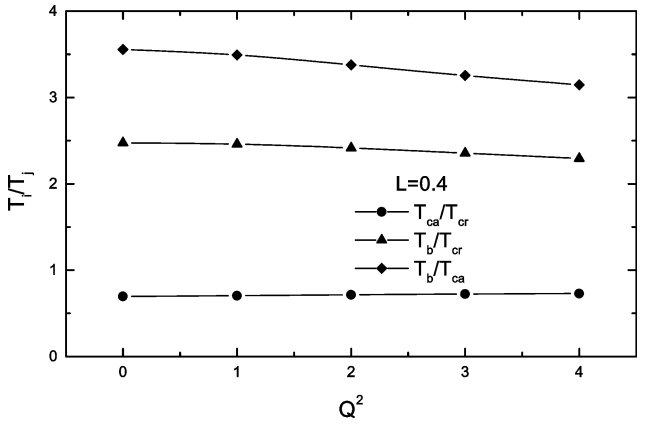

Fig. 7 Plot of different temperature ratios as a function of quadrupole moment for $L = 0.4$. T_{ca};temperature at which B_3 vanishes; T_{cr}, critical temperature; T_b, Boyle temperature.

ratio of the second virial coefficient to the molecular volume at the critical temperature is more or less a constant value of about ≈ -6.[34] This is a simple method that allows to give a first estimate of the critical temperature from knowledge of B_2 alone. If higher order virial coefficients are available, however, a much more sound approach consists in using the virial series as an equation of state, assuming that the critical point is inside the radius of convergence. Although the virial series is a low density expansion, so that this approach is questionable, it has been found that it is able to yield rather reasonable estimates for the critical properties. This idea was already explored by Barker *et al.*,[8] who used a virial series up to fifth order and predicted a critical temperature of $T_{cr} = 1.291$ for the Lennard-Jones fluid, in excellent agreement with computer simulation results.[35] This same idea has been used by other authors for non-spherical models such as dipolar hard spheres,[18] the Gay–Berne model[23] or different models of water.[20] However, the results are far less encouraging than those obtained by Barker *et al.*[8] The reason is that the latter authors were able to estimate up to the fifth virial coefficient, while for simple molecular systems, only virial coefficients up to the third were available. Boublik and Janecek have recently proposed a simple procedure to improve on the estimates obtained from the virial series truncated at the level of B_3.[24,25] The idea is to simply expand the series up to fourth order by employing the fourth virial coefficient of a hard repulsive body of similar shape.[10] We will now test the performance of both approximations. On the one hand, we consider an

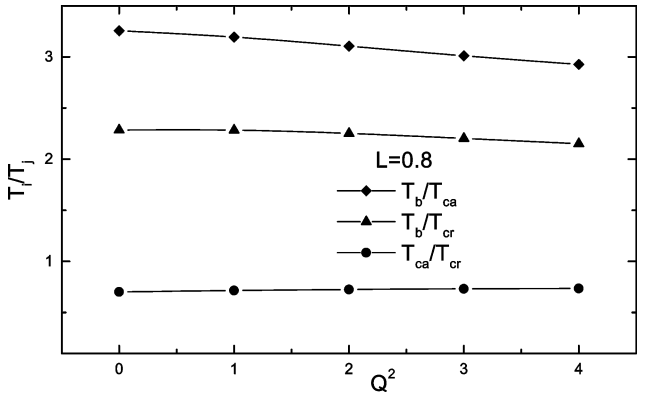

Fig. 8 Plot of different temperature ratios as a function of quadrupole moment for $L = 0.8$. T_{ca};temperature at which B_3 vanishes; T_{cr}, critical temperature; T_b, Boyle temperature.

Table 2 Results for T_{ca}, the temperature at which B_3 becomes zero, for all the models studied in this work

	Q^2				
L	0	1	2	3	4
0.0	0.90	1.14	1.62	2.21	2.96
0.2	2.98	3.05	3.23	3.46	3.72
0.4	2.20	2.25	2.37	2.52	2.69
0.5	1.93	1.98	2.07	2.20	2.35
0.6	1.72	1.77	1.85	1.96	2.09
0.8	1.44	1.49	1.56	1.66	1.77
1.0	1.27	1.33	1.41	1.51	1.65

equation of state obtained from the virial series, expanded up to third order, which we denote EOSB3:

$$\frac{p(\rho, T)}{k_B T} = \rho + B_2(T)\rho^2 + B_3(T)\rho^3 \qquad (2.12)$$

On the other hand, we will consider an approximate virial series expanded up to fourth order, which we denote EOSB4hb

$$\frac{p(\rho, T)}{k_B T} = \rho + B_2(T)\rho^2 + B_3(T)\rho^3 + B_4^{hb}\rho^4 \qquad (2.13)$$

where B_4^{hb} denotes the fourth virial coefficient of a nonpolar hard dumbbell, with bond length equal to L and diameter equal to σ. Within this approximation, we are assuming that the fourth virial coefficient of the quadrupolar diatomics is everywhere positive and depends neither on temperature nor on the quadrupole moment. For the lower order virial coefficients, however, we employ the numerical results obtained previously in ref. 26 for B_2 and in this work for B_3.

Once we have an approximation for the equation of state, the critical properties may be determined from the following thermodynamic conditions:

$$\begin{cases} \left(\dfrac{\partial p}{\partial V}\right)_{T_{cr}} = 0 \\ \left(\dfrac{\partial^2 p}{\partial V^2}\right)_{T_{cr}} = 0 \end{cases} \qquad (2.14)$$

In order to solve the above equations, we have fitted our results for B_3 according to the following equation, based on the exact form for the third virial coefficients of the square well fluid:[6]

$$B_3(T) = a_0 + a_1 x + a_2 x^2 + a_3 x^3 + a_4 x^4 + a_5 x^5 + a_6 x^6 \qquad (2.15)$$

where $x = \exp(\varepsilon/k_B T)$. The above equation provides an excellent fit for B_3 within the temperature range considered. As to B_2, we have employed a fit performed in previous work and available as ESI.[26] Finally, the fourth virial coefficients of hard diatomics required in EOSB4hb were taken from ref. 10. In units of the molecular volume, the required coefficients take the value $B_4/v^3 = 18.36$, 19.43, 20.35, 23.10, 27.61 and 34.52 for $L = 0.0$, 0.2, 0.4, 0.6, 0.8 and 1.0, respectively, where $v = \pi\sigma^3(2 + 3L - L^3)/12$.[10]

In Fig. 9 we plot critical temperatures of quadrupolar diatomics of different elongations as a function of quadrupole moment. The predictions of EOSB3 and EOSB4hb are compared with simulation results.[29] The figure shows that both predictions give reasonable results and correctly predict the qualitative trend of increasing critical temperature with increasing quadrupole. Predictions for the B4hb approximation are clearly superior, however. Both estimates are complementary, however, because they bracket the actual simulation results in all cases.

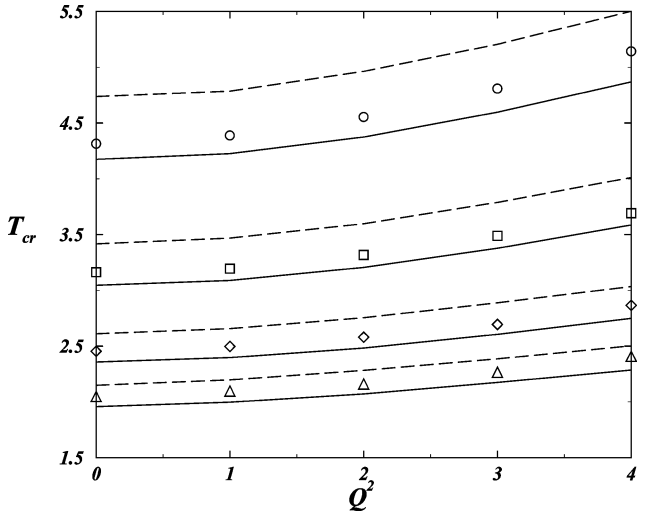

Fig. 9 Critical temperatures for different elongations as a function of the quadrupole moment. Symbols, simulation results from ref. 29 circles, $L = 0.2$; squares, $L = 0.4$; diamonds, $L = 0.6$; triangles, $L = 0.8$; The lines bracketing the simulation results are theoretical estimates from EOSB3 (dashed line) and EOSB4hb (full line).

The results for the critical pressure are shown in Fig. 10. Once more, the qualitative trends are correctly predicted by both approximations, but B4hb is seen to yield more accurate estimates. Again, the theoretical estimates bracket the simulation results in all cases, both for the three elongations shown in the figure and for all other elongations studied (not shown for the sake of clarity).

Despite the good agreement found for T_{cr} and p_{cr}, the agreement for the critical density is far less satisfying. Fig. 11 shows the critical densities for different elongations as a function of quadrupole. In this case, we only present results for two elongations, because otherwise the figure looks overcrowded. The models chosen show the general trend observed in all cases, however. It is found that the predictions for ρ_{cr} show a much larger error than for T_{cr} and p_{cr}. Although EOSB3 and EOSB4hb bracket the simulation results, as for the other critical properties, in this case the EOSB3 approximation is seen to be much better than EOSB4hb.

Given the relatively good agreement found for T_{cr} and p_{cr}, the failure of EOSB3 and EOSB4hb to give qualitatively similar predictions for ρ_{cr} may be understood as follows. By considering the virial series and solving for eqn. (2.14), it may

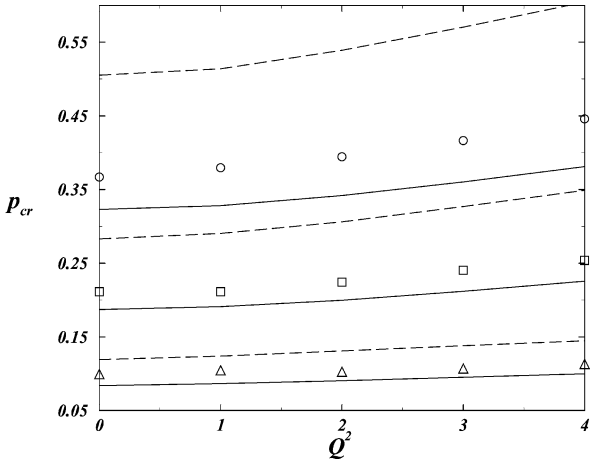

Fig. 10 As in Fig. 9 but for the critical pressure. Only results for $L = 0.2$, 0.4 and 0.8 are included.

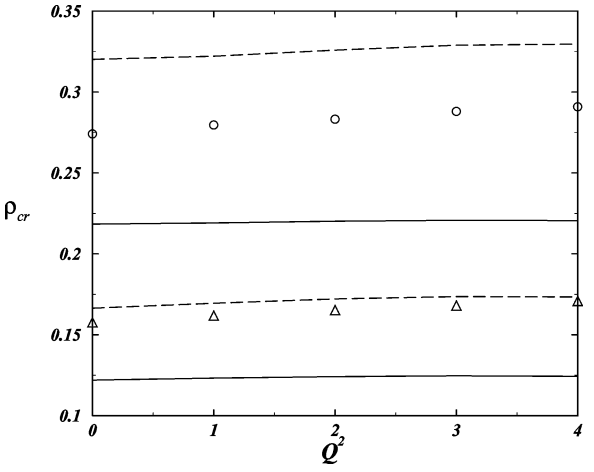

Fig. 11 As in Fig. 9 but for the critical density. Only results for $L = 0.2$ and 0.8 are included.

be shown that the compressibility factor at the critical point is approximately given by the following equation:[36–39]

$$Z_{\rm cr} = \frac{1}{3} + \mathrm{H}(k-3)\sum_{i=4}^{k} B_i/|B_2|^{i-1} \qquad (2.16)$$

where k stands for the order of the truncation, while H(l) is a Heaviside step function which vanishes for $l \leq 0$ and is unity for $l > 0$. From the above equation, it is seen that when the virial series is truncated at third order, $Z_{\rm cr} = 1/3$, independent of the actual value of the critical density and temperature, or of the temperature dependence of B_2 and B_3. This is qualitatively a reasonable approximation, since $Z_{\rm cr}$ is known to be quite insensitive to changes in the molecular properties. Quantitatively it is not a good guess, however, since experimentally one actually finds that $Z_{\rm cr}$ rarely exceeds 0.28. If we now consider that $T_{\rm cr}$ and $p_{\rm cr}$ are predicted accurately, then it must follow that one cannot give a good approximation for $\rho_{\rm cr}$, since $Z_{\rm cr}$ is far too large. As seen in Fig. 11, the problem is not improved by adding the fourth order term to the series, because B_4 is positive, and the overall effect is to increase the predicted value for $Z_{\rm cr}$, which was already too large. Indeed, for all the models studied we find that within this approximation $Z_{\rm cr}$ is always found inside the interval [0.345,0.355].

III. Conclusions

In this work we have performed numerical calculations for the third virial coefficient of quadrupolar Lennard-Jones diatomics. Our calculations include results for seven different elongations, $L = 0.0$, 0.2, 0.4, 0.5, 0.6, 0.8 and 1.0, and five different quadrupoles for each elongation, $Q^2 = 0$, 1, 2, 3 and 4. The study includes data over a temperature range between one half and twice the critical temperature of the models. The results for the virial coefficients of this work may be obtained as ESI.†

It is found that increasing the elongation at fixed quadrupole has the effect of increasing B_3. On the other hand, at fixed elongation B_3 first decreases with increasing quadrupole at low temperatures, then increases with increasing quadrupole at higher temperatures. In all cases, B_3 was found to change sign once within the temperature range considered. The temperature at which B_3 vanishes, $T_{\rm ca}$, is found to increase with the quadrupole moment at fixed elongation. It was also observed that $T_{\rm ca}$ is smaller than $T_{\rm cr}$, so that B_3 is positive at the critical point. Although both $T_{\rm cr}$ and $T_{\rm ca}$ increase with quadrupole moment, the ratio of these two temperatures is found to be rather insensitive to changes in Q^2.

We have also investigated the ability of the virial series to predict the critical properties of molecular fluids. Two different approximations have been considered. The first one (EOSB3) uses the exact second and third virial coefficients. The second one (EOSB4hb) approximates the fourth virial coefficient to that of a reference hard dumbbell, as suggested by Boublik and Janecek.[24,25] It is found that EOSB3 consistently over predicts T_{cr}, p_{cr} and ρ_{cr}. On the contrary, EOSB4hb consistently underestimates these properties. As a result, the two approximations are able to bracket the actual results from simulation in all cases. Furthermore, EOSB4hb gives results for T_{cr} and p_{cr} with an error of 5% or less. For ρ_{cr}, however, the agreement is far less satisfactory, with an error as large as 15%. Actually, in this case the EOSB3 approximation is found to give better predictions than EOSB4hb. The critical compressibility factor is over predicted by both approximations, though EOSB3 performs somewhat better. The accuracy of the predictions increases with elongation, because the longer the molecule, the lower the critical density, so that the virial series progressively becomes a better approximation.

An interesting point worth considering in future research is the extension of the methodology employed to estimate critical properties to the case of binary mixtures. The problem in this situation is perhaps more relevant, because there is a continuum of critical points, and measuring a limited number of crossed virial coefficients for the mixture would allow to estimate the whole critical line, at least for type I and type II phase diagrams.

Acknowledgements

Financial support is due to project number BFM-2001-1420-C02-01 and BFM-2001-1420-C02-02 of the Spanish MCYT (Ministerio de Ciencia y Tecnología). L.G. MacDowell would also like to thank the Universidad Complutense de Madrid and the spanish MCYT for the award of a Ramón y Cajal fellowship.

References

1 J. O. Hirschfelder, C. F. Curtiss, R. B. Bird, *Molecular Theory of Gases and Liquids*, John Wiley, New York, 1954.
2 D. A. McQuarrie, *Statistical Mechanics*, Harper & Row, New York, 1976.
3 J. E. Mayer and M. G. Mayer, *Statistical Mechanics*, John Wiley & Sons, New York, second ed., 1940.
4 W. Ameling, K. P. Shukla and K. Lucas, *Mol. Phys.*, 1986, **58**, 381–394.
5 R. Pospisil, A. Malijevsky and S. Labik, *Mol.Phys.*, 1988, **64**, 21–32.
6 J. A. Barker and J. J. Monaghan, *J. Chem. Phys.*, 1962, **36**, 2558–2563.
7 J. A. Barker and J. J. Monaghan, *J. Chem. Phys.*, 1962, **36**, 2564–2571.
8 J. A. Barker, P. J. Leonard and A. Pompe, *J.Chem.Phys.*, 1966, **44**, 4206–4211.
9 T. Kihara, vol. 5 of *Advances in Chemical Physics*, Wiley-Interscience, New York, 1963, pp. 147–188.
10 T. Boublik and I. Nezbeda, *Collect. Czech. Chem. Commun.*, 1986, **51**, 2301–2426.
11 M. H. Kalos, P. A. Whitlock, *Monte Carlo Methods*, John Wiley & Sons, New York, 1986, vol. 1.
12 L. G. MacDowell and C. Vega, *J. Chem. Phys.*, 1998, **109**, 5670–5680.
13 C. Vega, J. M. Labaig, L. G. MacDowell and E. Sanz, *J. Chem. Phys.*, 2000, **113**, 10 398–10 409.
14 W. Bruns, *Macromolecules*, 1984, **17**, 2826–2830.
15 K. Shida, K. Ohno, Y. Kawazoe and Y. Nakamura, *J. Chem. Phys.*, 2002, **117**, 9942–9946.
16 C. M. M. Duarte, C. Menduiña, A. Aguiar-Ricardo and M. N. da Ponte, *Phys. Chem. Chem. Phys*, 2002, **4**, 4709–4715.
17 A. Yethiraj and C. K. Hall, *Mol. Phys.*, 1991, **72**, 619–641.
18 C. Joslin and S. Goldman, *Mol. Phys.*, 1993, **79**, 499–514.
19 C. G. Joslin, C. G., S. Goldman, B. Tomberli and W. Li, *Mol. Phys.*, 1996, **89**, 489–503.
20 P. G. Kusalik, F. Liden and I. M. Svishchev, *J. Chem. Phys.*, 1995, **103**, 10 169–10 175.
21 B. Tomberli, S. Goldman and C. G. Gray, *Fluid Phase Equilib.*, 2001, **187–188**, 111–130.
22 T. Boublik, *Fluid Phase Equilib.*, 2001, **182**, 47–58.
23 E. de Miguel, L. F. Rull and K. E. Gubbins, *Physica. A*, 1991, **177**, 174–181.
24 J. Janecek and T. Boublik, *Mol. Phys.*, 2000, **98**, 93–99.
25 J. Janecek and T. Boublik, *Mol. Phys.*, 2000, **98**, 765–767.
26 C. Menduiña, C. McBride and C. Vega, *Phys. Chem. Chem. Phys*, 2001, **3**, 1289–1296.
27 C. Vega, C. McBride and C. Menduiña, *Phys. Chem. Chem. Phys*, 2002, **4**, 3000–3007.
28 T. Breitenstein and R. Lustig, *J. Mol. Liq.*, 2002, **98–99**, 261–282.
29 J. Stoll, J. Vrabec, H. Hasse and J. Fischer, *Fluid Phase Equilib.*, 2001, **179**, 339–362.
30 C. G. Gray, K. E. Gubbins, *Theory of Molecular Fluids*, Clarendon Press, Oxford, 1984.
31 T. Sun and A. S. Teja, *J. Phys. Chem.*, 1996, **100**, 17 365–17 372.
32 A. Yethiraj and C. K. Hall, *J. Chem. Phys.*, 1991, **95**, 8494–8506.
33 J. Vrabec, J. Stoll and H. Hasse, *J. Phys. Chem. B*, 2001, **105**, 12 126–12 133.
34 G. A. Vliegenthart and H. N. W. Lekerkerker, *J. Chem. Phys.*, 2000, **112**, 5364–5369.
35 A. Lotfi, J. Vrabec and J. Fischer, *Mol. Phys.*, 1992, **76**, 1319.
36 L. G. MacDowell, M. Müller, C. Vega and K. Binder, *J. Chem. Phys.*, 2000, **113**, 419–433.
37 C. Vega and L. G. MacDowell, *Mol. Phys.*, 2000, **98**, 1295–1308.
38 L. G. MacDowell, PhD thesis, Universidad Complutense de Madrid, 2000.
39 L. Lue, D. G. Friend and J. R. Elliott, Jr., *Mol. Phys.*, 2000, **98**, 1473–1477.